Experimental and theoretical study of the C$_4$ defect in neutron irradiated silicon

C. A. Londos,[a] D. N. Aliprantis, G. Antonaras, M. S. Potsidi, and T. Angeletos[a]

Solid State Physics Section, University of Athens, Panepistimiopolis, Zografos, Athens 157 84, Greece

This work reports infrared spectroscopy studies in neutron irradiated Cz-Si containing carbon. The material was thermally treated at high temperature prior to irradiation. The aim was to investigate the production and annealing of the C$_i$O$_i$(Si$_I$) defect, well-known as C$_4$ center. Besides the two standard localized vibrational modes (LVMs) at 934 and 1018 cm^{-1} detected always in room temperature measurements, another band was also detected at 760 cm^{-1}. The latter band has the same annealing behavior as the 934 and 1018 cm^{-1} bands. Its existence has been predicted by theoretical calculations previously, but it has not been reported definitely so far experimentally. The present study verifies unambiguously its presence. Upon annealing the above three bands begin to decay in the spectra at ~140 °C and disappear at ~200 °C. No other bands appear to arise in the spectra upon the disappearance of the above bands. Semi-empirical calculations of the LVM frequencies of the C$_4$ complex verify the correlation of the 760 cm^{-1} band with this center. The annealing kinetics of the bands was investigated, and it was found that their decay follows a second order reaction with an average activation energy of E ~ 0.50 ± 0.02 eV. *Published by AIP Publishing.* https://doi.org/10.1063/1.5024932

INTRODUCTION

In irradiated Cz-Si containing carbon, the main defects formed are oxygen-related and carbon-related complexes.[1,2] Regarding the latter family of defects, their formation sequence is as follows. The first produced defect is the C$_i$ formed via the Watkins replacement mechanism, where C$_s$ atoms turn to C$_i$ atoms by the capture of self-interstitials (Si$_I$) produced by the irradiation. The C$_i$ defect has been detected by electrical and optical techniques, and a number of signals have been associated with it. Thus, two deep levels[3,4] at E$_v$ + 0.28 eV and E$_c$ − 0.10 eV (DLTS studies), two orthorhombic signals[4,5] labeled G-12 and Si-L6 (EPR studies), two absorption lines[6] at 922 and 932 cm^{-1} (FTIR studies), and a zero-phonon[7] line at 856 meV (PL studies) have been associated with the C$_i$ defect.

At room temperature, C$_i$ defect is mobile and pairs with carbon and oxygen to form the C$_i$C$_s$ and the C$_i$O$_i$ pairs, respectively. C$_i$O$_i$ defect has also been detected by many experimental techniques. Thus, a deep level[8] at E$_v$ + 0.38 eV (DLTS studies), a monoclinic-I signal[9] labeled G-15 (EPR studies), several absorption lines at 529, 540, 550, 585, 742, 865, 1116 cm^{-1} (FTIR studies),[2,10,11] and a zero-phonon[2,12] line at 790 meV (PL studies) have been associated with the C$_i$O$_i$ defect. At high irradiation doses, some of the created self-interstitials that survive annihilation are trapped by the C$_i$, C$_i$C$_s$, and C$_i$O$_i$ leading to the formation of larger complexes[2,10–15] as C$_i$(Si$_I$)$_n$, C$_i$C$_s$(Si$_I$)$_n$, and C$_i$O$_i$(Si$_I$)$_n$ with n = 1,2…. Numerical modeling of defect evolution[12,16–18] has been used to understand and explain optical absorption spectra in irradiated silicon and predict defect concentration and their evolution in an attempt to improve the quality of certain devices, for instance radiation detectors.

The first member of the last family is the C$_i$O$_i$(Si$_I$) complex. In contrast with the C$_i$ and C$_i$O$_i$ defects which have been detected by many experimental techniques, the C$_i$O$_i$(Si$_I$) has been detected only by IR spectroscopy and two absorption bands[2,10,12] at 934 and 1018 cm^{-1} (in RT measurements) have been associated with this complex. No DLTS, EPR, and PL signals have been reported so far for this center. In any case, the picture regarding the C$_i$O$_i$(Si$_I$) defect is far for been complete. There are questions about the structure, the electrical activity, the number of the relative localized vibrational modes (LVMs), and the evolution of the defect upon thermal anneals. Regarding the geometry of the C$_4$ defect, at least three configurations have been studied.[19,20] In the two of them C$_4$(a) and C$_4$(c) the oxygen atom is trivalent although in the other one C$_4$(b) is divalent. The latter configuration for the C$_i$O$_i$(Si$_I$) defect is also suggested[21] in another work pointed out that the C$_4$ structure is similar to the O form of the C$_i$O$_i$H complex.[22] On the other hand, other studies[23] concluded in favor of the C$_4$(a) and C$_4$(c) configurations of the defect. Regarding the electrical activity, the theoretical studies have found[19,20] that all the three configurations C$_4$(a), C$_4$(b), and C$_4$(c) should introduce deep levels in the gap, although there is no experimental evidence reported so far. This absence of electrical activity attracts attention, since as has been earlier pointed out[19] the C$_i$O$_i$(Si$_I$) structure comprising C$_i$, O$_i$, and (Si$_I$) is expected to be electrically active. Regarding the optical activity of the C$_4$ defect, although theoretical studies[19,20] have correlated several LVMs with the three geometries C$_4$(a), C$_4$(b), and C$_4$(c) of the defect; however, at low temperature measurements, only two IR bands at 940 and 1024 cm^{-1} have been detected experimentally and positively associated so far with the C$_4$ complex. This point is very interesting since the C$_i$O$_i$(Si$_I$) defect forms by the addition of a (Si$_I$) to the C$_i$O$_i$ pair which has at least seven LVMs and one expects a similar number of LVMs to be connected

[a]Electronic addresses: hlontos@phys.uoa.gr and angelet@phys.uoa.gr

with the $C_iO_i(Si_I)$ structure. It should be noted that a band at 753 cm^{-1}, which is among the theoretically predicted LVMs related to the C_4 complex, has arisen[20] questions why has not been detected so far experimentally. Regarding the annealing behavior of the C_4 defect, there are also controversial points in the literature. In low temperature measurements, the defect seems to convert[24,25] upon annealing to three different configurations with relative IR bands connected with its configuration although the bands of the two last configurations are not detected in room temperature measurements. There are two aspects regarding this behavior. It has been suggested[24] that when the annealing temperature increases, the defect successively transforms to more stable configurations of the $C_iO_i(Si_I)$ structure. These configurations are detected at low temperature measurements with certain IR signals related to them, correspondingly. In another way of explanation, it was suggested[25] that upon increasing the temperature the C_4 defect captures self-interstitials and successively transforms to larger structures[2,13] $[C_iO_i(Si_I) \rightarrow C_iO_i(Si_I)_2 \rightarrow C_iO_i(Si_I)_3 \rightarrow C_iO_i(Si_I)_4]$, where $C_iO_i(Si_I)_2$ exhibits metastability. On low T measurements, the $C_iO_i(Si_I)_2$ give rise to certain bands, although on measurements at room temperature the defect has been converted[25] to another configuration with no detectable IR bands.

Evidently, there are a lot of points regarding the properties and behavior of the C_4 defects that need further elaboration. In this work, we have performed neutron irradiations in initially heat treated Cz-Si containing C, on the purpose to enhance the intensity of the relative signals in order to investigate the existence of additional IR bands of the $C_iO_i(Si_I)$ complex. Indeed, as a result of the thermal treatment at high temperature of Cz-Si, extended defects form as oxygen precipitates, as, for instance, rod-like defects and dislocations.[26–29] Importantly, Si_Is are emitted in the course of the precipitation to accommodate for the volume shortage associated with this process. These Si_Is are captured in the periphery of the oxygen precipitates and the Si matrix.[29–31] In the course of irradiation, some of the trapped Si_Is are liberated and this interface region could act as additional source of Si_Is. This leads to an enhancing production of defects involving the participation of Si_Is in their formation process, for instance, carbon-oxygen related defects. Thus, besides the 934 and 1018 cm^{-1} bands of the C_4 defect, another one at 760 cm^{-1} was also seen in our spectra. It has the same annealing behavior with the other two bands. The kinetics that describes the decay of the above three bands was also investigated and certain conclusions were reached about the involved reactions. Additionally, semi-empirical calculations were performed in order to estimate the LVM frequencies of the $C_iO_i(Si_I)$ defect.

EXPERIMENTAL DETAILS

Cz-Si samples of 2 mm thickness with oxygen and carbon concentrations of 7.2×10^{17} and 1.52×10^{17} cm^{-3}, respectively, were used. They were initially subjected to thermal treatments at 1000 °C for 5h. Then, they were irradiated with 5 MeV fast neutrons at fluence of 1×10^{17} n cm^{-2}, at ∼40 °C. After irradiation, the samples were subjected to isochronal anneals of 20 min duration with the annealing
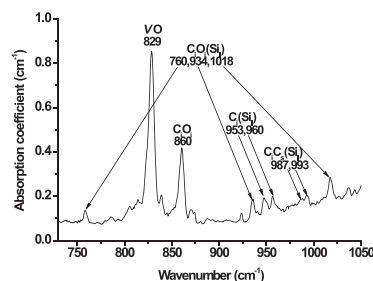

FIG. 1. Segments of the IR spectra for the thermally treated, neutron-irradiated Cz-Si sample.

temperature to increase ∼10 °C in each measurement. During the anneals, the samples were put in quartz cells and the whole set was inserted in a quartz tube, to avoid contamination with the walls of the furnace. Infrared spectroscopy measurements were carried out at room temperature after each annealing stage, with a Jasco-IR 700 dispersive spectrometer. The spectral resolution was 1 cm^{-1}. The two-phonon absorption was always subtracted by using a reference sample of FZ-Si material of equal thickness.

RESULTS AND DISCUSSION

Figure 1 exhibits segments of the IR spectra after the high temperature (HT) at 1000 °C and the subsequent irradiation in the frequency range of 750 to 1050 cm^{-1}. The well-known bands of the VO (829 cm^{-1}), C_iO_i (860 cm^{-1}), $C_iO_i(Si_I)$ (934, 1018 cm^{-1}), $C_i(Si_I)$ (953, 960 cm^{-1}), and $C_iC_s(Si_I)$ (987, 993 cm^{-1})[14] defects are present in the spectra, as well as a band at 760 cm^{-1}. Notably, the wavenumbers of defects detected by us are generally less by 1–2 cm^{-1} than those in the literature. We hope that these shifts do not cause problems in the other researchers in the field. In any case, such values from our group have already been published.[14,15] Another point: Regarding $C_iC_s(Si_I)$ (987, 993 cm^{-1}), previous research[11] has assigned these frequencies to $C_iO_i(Si_I)_2$ and $C_iO_i(Si_I)_3$ complexes, respectively. Apparently, the two assignments are in disagreement and we expect that future research would shed new light on this issue.

Figure 2 shows the thermal evolution of the 934, 1018 cm^{-1} bands of the $C_iO_i(Si_I)$ defect, as well as the
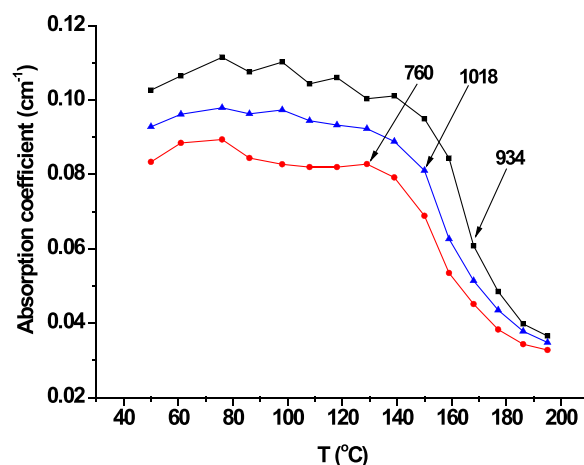

FIG. 2. Thermal evolution of the 760, 934, and 1018 cm^{-1} bands.

evolution of the 760 cm^{-1} band, in the course of the isochronal anneals. The three bands begin to decay at ∼140 °C and disappear together just below ∼200 °C, without the concomitant growth of other bands in the spectra in the course of their disappearance. This is an indication of a common origin of the bands. Additionally, there are theoretical calculations[19,20] predicting the existence of a band around 753 cm^{-1} originated from the $C_iO_i(Si_I)$ center. In an attempt to correlate our 760 cm^{-1} experimental band with the C_4 complex, it would be necessary to calculate the activation energies of the three bands. To do this, we have to study the annealing kinetics that governs the reactions which describe the decay of the above three bands. Thus, it is necessary to determine the order of these reactions. To this end, we suppose that they follow a γ-order kinetics described by the following equation:

$$\frac{d[C]}{dt} = -k_\gamma[C]^\gamma, \qquad (1)$$

where [C] is the concentration of the defect and k_γ the rate constant. Next, we shall try to calculate the value of γ that fits best with the experimental data. Equation (1) leads to the following expressions[32–34] of k_γ:

$$k_\gamma\Delta t = \ln\frac{[C]_t}{[C]_{t+\Delta t}}, \quad \text{for } \gamma = 1, \qquad (2)$$

$$k_\gamma\Delta t = \frac{1}{[C]_t^{\gamma-1}} - \frac{1}{[C]_{t+\Delta t}^{\gamma-1}}, \quad \text{for } \gamma \neq 1. \qquad (3)$$

Through Eqs. (2) and (3), we can receive values of the rate constant k_γ for each annealing temperature T. Of course, these values change with the value of the reaction order γ. For each value of γ, the activation energy E_γ of the process can be calculated by making the Arrhenius plot $\ln(k_\gamma) = f(1/T)$. This is a straight line with a slope E_γ/k_B, where k_B is the Boltzmann constant. The next step is to find the proper value of γ that describes the kinetics of the experiment data. To this end, we calculate the correlation coefficient r_γ of the linear regression for any value of γ, which is defined[35] by the expression

$$r_\gamma = \frac{n\sum\frac{1}{T}\ln(k_\gamma) - \sum\frac{1}{T}\sum\ln(k_\gamma)}{\sqrt{\left[n\sum\left(\frac{1}{T}\right)^2 - \left(\sum\frac{1}{T}\right)^2\right]\left[n\sum(\ln(k_\gamma))^2 - \left(\sum\ln(k_\gamma)\right)^2\right]}}, \qquad (4)$$

where n is the number of points used in the regression. The most acceptable value of γ is that for which r_γ becomes maximum.[32]

Figure 3 is a plot of the correlation coefficient r_γ of γ for the three bands 760, 934, and 1018 cm^{-1}. As it is immediately seen, the maximum value of r_γ for all these bands is obtained for γ around 2, indicating that the main reaction describing the decay of the bands is of second order. Thus, for our case with $\gamma = 2$, expression (3) becomes

$$\left[k_2\Delta t = \frac{1}{[C]_t} - \frac{1}{[C]_{t+\Delta t}}\right],$$

which is better written as

$$k_2\tau = \frac{1}{[C']} - \frac{1}{[C]_o}, \qquad (5)$$

where k_2 has a temperature dependence of the form $k_2 \propto e^{-E/k_B T}$, E being the activation energy of the process, k_B the Boltzmann constant, $[C]_o$ the initial concentration of the defect, and $[C']$ the concentration of the defect after annealing for time τ, at temperature T. Thus, by fitting $\ln k_2$ versus $1/T$ in the range 160–200 °C, where the experimental data follow the best Arrhenius fitting (Fig. 4), we found similar activation energies for the three bands, that is, $E_{760} = 0.46$ eV, $E_{934} = 0.50$ eV, and $E_{1018} = 0.52$ eV, a further supporting element that the bands originate from the same center, the $C_iO_i(Si_I)$ defect. The average activation energy of the bands is ∼0.50 ± 0.02 eV. Our results suggest the following annealing reaction: $C_iO_i(Si_I) + (Si_I) \rightarrow C_iO_i(Si_I)_2$. Importantly, according to recent studies,[25] the $C_iO_i(Si_I)_2$ is not expected to be detected in room temperature measurements in agreement with the present results, where no signals arise in the spectra when $C_iO_i(Si_I)$ bands annealed out.

Calculation of the LVM frequencies by the semi-empirical method

In order to calculate the oscillation frequencies (LVMs) of a complex, we shall use a previously presented[36] semi-empirical method. In this method, we assume that the complex consists of two distinct defects in close proximity. Apparently, the LVM frequencies of these two individual defects are modified within the complex. To calculate the modified frequencies, we consider that each one defect oscillates near the minimum of a power-law potential[36,37]

$$U(r) = 4\varepsilon\left[\left(\frac{\sigma}{r}\right)^n - \left(\frac{\sigma}{r}\right)^m\right]. \qquad (6)$$

The positive and negative parts in Eq. (6) refer to the repulsing and attractive interaction, respectively, ε is the absolute value of the potential $U(r)$ at the equilibrium position r_o of the vibrating defect atom and $\sigma = \frac{\sqrt{2}}{2}r_o$. For the case of a covalent bond,[37] $n = 4$ and $m = 2$.
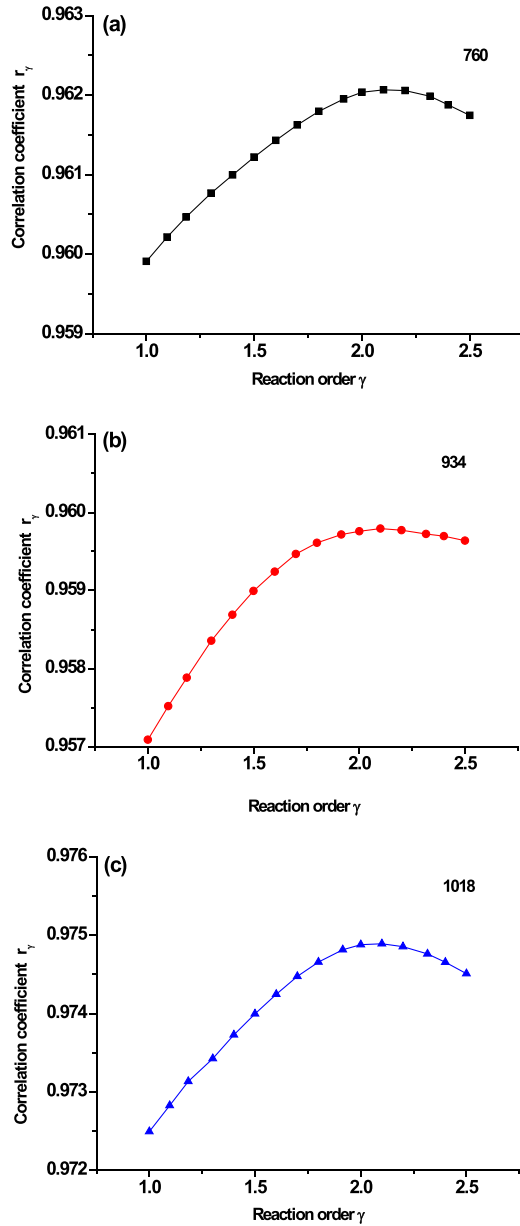
FIG. 3. Correlation coefficient versus reaction order for the (a) 760, (b) 934, and (c) 1018 cm^{-1} bands.
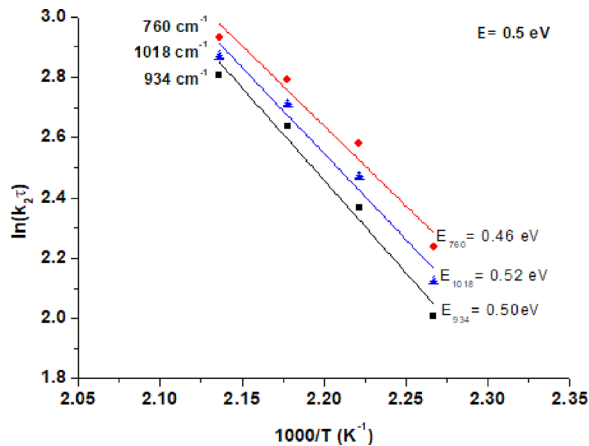

FIG. 4. Arrhenius plots for the decay of the 760, 934, and 1018 cm^{-1} bands.

The modification of the attractive part of the potential can be described by the introduction of a parameter λ

$$U(r) = 4\varepsilon \left[\left(\frac{\sigma}{r}\right)^4 - (1+\lambda)\left(\frac{\sigma}{r}\right)^2 \right]. \quad (7)$$

By setting the first derivative of the potential energy, at the equilibrium position, equal to zero, we find from Eq. (7) that

$$r = \sigma \sqrt{\frac{2}{1+\lambda}}. \quad (8)$$

Next, calculating the second derivative at the equilibrium position we find

$$\left.\frac{d^2U}{dr^2}\right|_{r_0} = \frac{4\varepsilon}{\sigma^2}(1+\lambda)^3. \quad (9)$$

Since this second derivative equals the force constant, the latter being proportional to the square of the vibrational frequency, we can write

$$\omega = \alpha\Omega, \quad (10)$$

where Ω is the frequency of each individual defect and ω is the modified one within the complex structure. Parameter a is related to λ by the expression

$$\alpha = (1+\lambda)^{3/2}. \quad (11)$$

The bond energy[36,38] can be written as

$$E_{bond} = V_2(1 - \alpha_m), \quad (12)$$

where V_2 is the covalent energy and α_m the metallicity.[36] Metallicity measures[38,39] the metallic character of a covalent bond.

We shall suppose that the energy in Eq. (12) comes from the power law potential

$$U_\zeta(r) = 4\varepsilon \left[\left(\frac{\sigma}{r}\right)^4 - (1-\zeta)\left(\frac{\sigma}{r}\right)^2 \right], \quad (13)$$

where ζ is a parameter that measures the effect of metallicity.[36,38] From Eq. (13), we get the following expression at the equilibrium:

$$E_{bond} = \varepsilon(1 - \zeta)^2. \quad (14)$$

By comparing Eqs. (12) and (14), we find

$$\zeta = 1 - \sqrt{1 - \alpha_m}. \quad (15)$$

When impurities are present in the lattice, the metallicity of the silicon atoms that bond with these impurities is expected to change and reasonably an average value $\langle\alpha_m\rangle$ should be considered. Now, let us represent ζ_i and ζ_f the initial and final values of the ζ parameter, as well as $\langle\alpha_m\rangle_i$ and $\langle\alpha_m\rangle_f$ the appropriate average values of the metallicity of a silicon atom before and after the introduction of the impurity, then the difference

$$\zeta_f - \zeta_i = \left(1 - \sqrt{1 - \langle\alpha_m\rangle_f}\right) - \left(1 - \sqrt{1 - \langle\alpha_m\rangle_i}\right) \quad (16)$$

can be seen as the change in the attractive part of the potential for the Si atom with respect to the perturbation introduced by the impurity atom.

Then, by calculating the corresponding metallicities $\langle\alpha_m\rangle_i$ and $\langle\alpha_m\rangle_f$ for a certain defect complex, we can find the λ parameter and therefore the a parameter. Thus, from Eq. (10), as described below, we can finally calculate the frequencies ω of the complex.

Calculation of the frequency of the C₄ complex

In order to calculate the LVMs of the $C_iO_i(Si_I)$ defect, it is necessary to determine the most possible structure of the defect. As we mentioned earlier, three different configurations for the $C_iO_i(Si_I)$ defect, labeled C4(a), C4(b), and C4(c) have been proposed.[19] In the C4(a) and C4(c) configurations, the oxygen atom is threefold coordinated, while in the C4(b) configuration, it is twofold coordinated. All three configurations[19] have LVMs that could be consistent with the observed bands at $934\,cm^{-1}$ (C-related) and $1018\,cm^{-1}$ (O-related) at room temperature measurements,[10] as well as the new band reported here at $760\,cm^{-1}$. The highest O-related frequency for a trivalent oxygen atom in the $C_iO_i(Si_I)$ defect [configurations C4(a) and C4(c)] is calculated in the range of $\sim750\,cm^{-1}$ [indeed, $753\,cm^{-1}$ for C4(a) and $763\,cm^{-1}$ for C4(c)].[19] This is also the case for the C_iO_i defect,[22] with its oxygen atom also being threefold coordinated, and for which the highest O-related band is found at $742\,cm^{-1}$. Notably, the $742\,cm^{-1}$ band of the C_iO_i defect is unusually broad, with a $\sim10\,cm^{-1}$ full width at half maximum.[22] Reasonably, one should expect that a threefold coordinated atom in the $C_iO_i(Si_I)$ defect would also have its $\sim750\,cm^{-1}$ band very broad. Now, the $1018\,cm^{-1}$ (O-related) band in the configurations C4(a) and C4(c) is a combination mode[19] of two bands, one at $\sim750\,cm^{-1}$ and the other at $\sim250\,cm^{-1}$. Since the $\sim750\,cm^{-1}$ band is expected to be very broad, the combination mode at $1018\,cm^{-1}$ would be also very broad. However, the width of the $1018\,cm^{-1}$ band is small $\sim4.7\,cm^{-1}$ (Fig. 1). Thus, $1018\,cm^{-1}$ band could not be related to the C4(a) and C4(c) configurations. Therefore, it seems more reasonable that the most probable structure of the $C_iO_i(Si_I)$ defect is that of configuration C4(b), with a twofold oxygen atom. A similar structure, with a divalent oxygen atom, has also been proposed by Davies *et al.*[21]

The $C_iO_i(Si_I)$ defect with a divalent oxygen atom (Fig. 5) could be considered as a $C_i(Si_I)$ defect being next to an interstitial oxygen atom. The O_i defect has a well-known band[1] at $1107\,cm^{-1}$ at room temperature related to its stretching mode, although the $C_i(Si_I)$ defect has two bands[14] at 960 and $953\,cm^{-1}$. We see that the $934\,cm^{-1}$ (C-related) band of the $C_iO_i(Si_I)$ is very close to those of the $C_i(Si_I)$ defect. It can be considered that this mode of $C_iO_i(Si_I)$ defect is almost unaffected by the presence of interstitial oxygen. This is probably due to the fact that the direction of oscillation of this mode is perpendicular to the direction of the
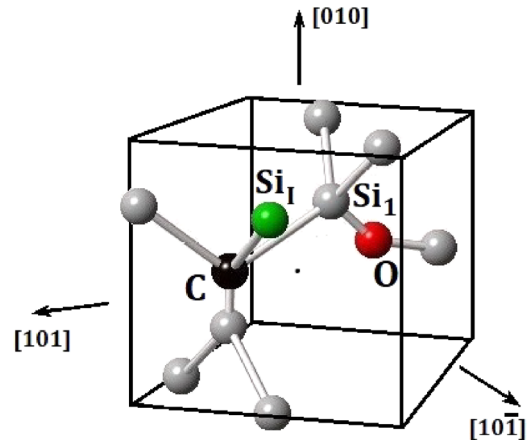

FIG. 5. The structure of the $C_iO_i(Si_I)$ defect in the C4(b) configuration.

oscillation of the stretching mode of O_i defect. Indeed, since the force constants of the stretching modes are, in general, many times greater than the force constants of the bending modes which are related to changes in angles, a vertical perturbation of this oscillation mode would not much affect its frequency.

The other two modes, $1018\,cm^{-1}$ (O-related) and $760\,cm^{-1}$ (C-related), can be seen as perturbed oscillation modes of $1107\,cm^{-1}$ (stretching mode of O_i) and $953\,cm^{-1}$ (or $960\,cm^{-1}$) of the $C_i(Si_I)$ defect, respectively.

In what follows, we apply the method described above for the case of the C_4 defect. The carbon atom is surrounded by four Si atoms, one of which (let it call Si1) is positioned between the carbon and the oxygen atom (Fig. 5). The latter atom has two neighbor Si atoms (one of which is Si1).

Let Ω_O ($=1107\,cm^{-1}$) be the frequency of the O_i defect which is modified within the C_4 structure to ω_O. Next, we shall calculate ω_O theoretically and compare it with the experimental value at $1018\,cm^{-1}$ of the C_4 defect. Similarly, let the Ω_C ($=953\,cm^{-1}$ or $960\,cm^{-1}$) be the frequency of the $C_i(Si_I)$ which is modified within the C_4 defect to ω_C. We shall also calculate ω_C theoretically and compare it with the experimental value at $760\,cm^{-1}$ of the C_4 defect.

We note that the metallicity of silicon has a value of 0.81 (Table I in Ref. 38). In the case of oxygen impurity in silicon, the Si-O bond is much less metallic than Si-Si bond,[36,39] and therefore its contribution to the metallicity of the Si1 is negligible. Thus, the metallicity for the Si1 atom will be given by the relation

$$\langle\alpha_m\rangle_{i,O} = \frac{3 \times 0.81 + 1 \times 0}{4} = 0.6075. \quad (17)$$

In the case of carbon impurity in silicon, the metallicity of Si-C bond is logical to be taken equal to the average of the metallicity of the Si-Si bond ($a_m = 0.81$) and of the C-C bond ($a_m = 0.40$) (Table I in Ref. 38), that is, $(0.81 + 0.40)/2 = 0.162$. Thus, the metallicity of the Si1 silicon atom will be given by the relation

$$\langle\alpha_m\rangle_{i,C} = \frac{3 \times 0.81 + 1 \times \dfrac{0.81 + 0.40}{2}}{4} = 0.7588. \quad (18)$$

The metallicity of Si1 within the C_4 defect is

$$\langle \alpha_m \rangle_f = \frac{2 \times 0.81 + 1 \times \dfrac{0.81 + 0.40}{2} + 1 \times 0}{4} = 0.5563, \tag{19}$$

and from Eq. (16) for the case of oxygen we find

$$\zeta_f - \zeta_{i,O} \approx -0.0396, \tag{20}$$

while for the case of C we find

$$\zeta_f - \zeta_{i,C} \approx -0.1750. \tag{21}$$

Since the stretching mode of the O_i defect is oriented towards the two silicon atoms which are bonded to the oxygen atom, one can write[36]

$$\lambda_O = \frac{\zeta_f - \zeta_{i,O}}{2} \approx -0.0198. \tag{22}$$

Although the carbon atom is surrounded by four silicon atoms rather than two, the relation (24) can also hold for the case of the carbon atom

$$\lambda_C = \frac{\zeta_f - \zeta_{i,C}}{2} \approx -0.0875. \tag{23}$$

This can be explained by the fact that force constants for the stretching modes are, in general, many times greater than the force constants related to bending modes and therefore the overall contribution of the Si–C bonds can be considered, for the purposes of this semi-empirical model, as having the same effect as the rather linear Si–O–Si oxygen defect.

Thus, substituting these values of λ_O and λ_C in Eq. (11), we find the corresponding values of parameters a_O and a_C and, consequently, from Eq. (10) we finally get $\omega_O = 1074\,\text{cm}^{-1}$ and $\omega_C = 829\,\text{cm}^{-1}$ (or $837\,\text{cm}^{-1}$), respectively. These values are quite close to the experimental values $1018\,\text{cm}^{-1}$ and $760\,\text{cm}^{-1}$, respectively (the errors are only $\sim 6\%$ and $\sim 9\%$, respectively).

In the recent years, advanced theoretical methods employing, for instance, density functional calculations (DFT) were usually used[19,21] to determine the structure and the LVM frequencies of defects. In our study, we have approached the issue from another point of view, as analytically described earlier, by taking into account the vibrational frequencies of the individual constituents of a defect and calculating their changes when participating in the defect structure, thus allowing the calculation of the frequencies of the defect. This method is apparently less strict than those involving DFT calculations; however, it manages to determine all the experimentally detected frequencies of the C_4 complex. Possible sources of errors in our method may be the following. At first, the change in the attractive part of $U(r)$ [Eq. (7)] is expressed by the insertion of the parameter λ. However, this is a first order approximation, although the real correction is certainly more complicated. Second, there is an error in the way we calculate the term metallicity a_m. This quantity is calculated approximately, since we use an average value of it.

Indeed, in our calculations, we assumed that each bond contributes equivalently to the average value of metallicity.

CONCLUSIONS

In the present work, we have performed experimental and theoretical studies to investigate the $C_iO_i(Si_I)$ complex in irradiated Si. The combination of thermal pre-treatment and neutron irradiation facilitated the detection of weak signals arisen from the defect that otherwise may be missed in RT measurements. Thus, by using IR spectroscopy, we detected an additional band at $\sim 760\,\text{cm}^{-1}$ which showed the same evolution and annealing kinetics with the other two band at 934 and $1018\,\text{cm}^{-1}$ of the $C_iO_i(Si_I)$ defect. This is a strong indication that $760\,\text{cm}^{-1}$ band originates also from the $C_iO_i(Si_I)$ defect. Furthermore, their decay follows a second order reaction with an activation energy of E $\sim 0.50 \pm 0.02\,\text{eV}$. This suggests the reaction $C_iO_i(Si_I) + Si_I \rightarrow C_iO_i(Si_I)_2$, in agreement with our previous results. Semi-empirical calculations gave a significant support in this assignment and more over suggested that the most probable configuration of the $C_iO_i(Si_I)$ defect is that evolving a divalent oxygen atom in the structure.

ACKNOWLEDGMENTS

[1] C. A. Londos, L. G. Fytros, and G. J. Georgiou, Defect Diffus. Forum **171–172**, 1 (1999).
[2] G. Davies and R. C. Newman, in *Handbook on Semiconductors, Materials, Properties and Preparations*, edited by T. S. Moss and S. Mahajan (Elsevier, North-Holland, Amsterdam, 1994), Vol. 3b, p. 1557.
[3] L. C. Kimerling, M. T. Assom, J. L. Benton, P. J. Drevinsky, and C. E. Caefer, Mater. Sci. Forum **38–41**, 141 (1989).
[4] L. W. Song and G. D. Watkins, Phys. Rev. B **42**, 5759 (1990).
[5] G. D. Watkins and K. L. Brower, Phys. Rev. Lett. **36**, 1329 (1976).
[6] A. R. Bean and R. C. Newman, Solid State Commun. **8**, 175 (1970).
[7] P. Leary, R. Jones, S. Oberg, and V. J. B. Torres, Phys. Rev. B **55**, 2188 (1997).
[8] P. M. Mooney, L. J. Cheng, M. Suli, G. D. Gerson, and J. W. Corbett, Phys. Rev. B **15**, 3836 (1977).
[9] J. M. Trombetta and G. D. Watkins, Appl. Phys. Lett. **51**, 1103 (1987).
[10] C. A. Londos, M. S. Potsidi, G. D. Antonaras, and A. Andrianakis, Physica B **376–377**, 165 (2006).
[11] L. I. Murin, V. P. Markevich, J. L. Lindstrom, M. Kleverman, J. Hermansson, T. Hallberg, and B. G. Svensson, Solid State Phenom. **82–84**, 57 (2002); J. Coutinho, R. Jones, P. R. Briddon, S. Oberg, L. I. Murin, V. P. Markevich, and J. L. Lindstrom, Physica B **308–310**, 305 (2001).
[12] G. Davies, E. C. Lightowlers, R. C. Newman, and A. S. Oates, Semicond. Sci. Technol. **2**, 524 (1987).
[13] S. P. Chappell and R. C. Newman, Semicond. Sci. Technol. **2**, 691 (1987).
[14] C. A. Londos, M. S. Potsidi, and E. Stakakis, Physica B **340–342**, 551 (2003).
[15] M. S. Potsidi and C. A. Londos, J. Appl. Phys. **100**, 033523 (2006).
[16] B. C. MacEvoy and G. Hill, Mater. Sci. Semicond. Process. **3**, 243 (2000).
[17] M. Huhtinen, Nucl. Instrum. Methods Phys. Res., Sect. A **491**, 194 (2002).
[18] G. Davies, Mater. Sci. Forum **38–41**, 151 (1989).
[19] D. J. Backlund and S. K. Estreicher, Phys. Rev. B **77**, 205205 (2008).
[20] D. J. Backlund and S. K. Estreicher, Physica B **401–402**, 163 (2007).
[21] G. Davies, S. Hayama, S. Hao, B. B. Nielsen, J. Coutinho, M. Sanati, S. K. Estreicher, and K. M. Itoh, Phys. Rev. B **71**, 115212 (2005).
[22] J. Coutinho, R. Jones, P. R. Briddon, S. Oberg, L. I. Murin, V. P. Markevich, and J. L. Lindstrom, Phys. Rev. B **65**, 014109 (2001).

[23]H. Wang, A. Chroneos, C. A. Londos, E. N. Sgourou, and U. Schwingensclogl, Sci. Rep. **4**, 4909 (2014).

[24]L. I. Murin, J. L. Lindstrom, G. Davies, and V. P. Markevic, Nucl. Instrum. Methods Phys. Res., Sect. B **253**, 210 (2006).

[25]T. Angeletos, A. Chroneos, and C. A. Londos, J. Appl. Phys. **119**, 125704 (2016).

[26]H. Bender and J. Vanhellemont, in *Handbook on Semiconductors, Materials, Properties and Preparations*, edited by T. S. Moss and S. Mahajan (Elsevier, North-Holland, Amsterdam, 1994), Vol. 3b, p. 1637.

[27]A. Borghesi, B. Pivac, A. Sassella, and A. Stella, J. Appl. Phys. **77**, 4169 (1995).

[28]R. C. Newman, J. Phys.: Condens. Matter **12**, R335 (2000).

[29]U. Gosele, *Oxygen, Carbon, Hydrogen and Nitrogen in Silicon* (Mater. Res. Soc. Symp. Proc., 1986), Vol. 59, p. 419.

[30]R. C. Newman, *Defects in Electronic Materials* (Mater. Res. Soc. Symp. Proc., 1988), Vol. 104, p. 25.

[31]H. Bender and J. Vanhellemont, *Defect Engineering in Semiconductor Growth, Processing and Device Technology* (Mater. Res. Soc. Symp. Proc., 1992), Vol. 262, p. 15.

[32]S. Ishino, F. Nakazawa, and R. Hasiguti, J. Phys. Chem. Solids **24**, 1033 (1963).

[33]P. W. Atkins, *Physical Chemistry* (Oxford University Press, 1994).

[34]K. J. Laidler, *Chemical Kinetics* (Harper & Row, New York, 1987).

[35]E. Grow, F. Davis, and M. Maxfield, *Statistical Manual* (Dover, New York, 1960), pp. 157–158.

[36]C. A. Londos, N. Sarlis, L. G. Fytros, and K. Papastergiou, Phys. Rev. B **53**, 6900 (1996).

[37]W. Harrison, *Electronic Structure and the Properties of Solids* (Dover, New York, 1989).

[38]W. Harrison, Phys. Rev. B **27**, 3592 (1983).

[39]S. Pantelides and W. Harrison, Phys. Rev. B **13**, 2667 (1976).